100W class green 10ps 280µJ laser with M^2<1.4 using Z-slab amplifier

Simon P. Chard[*a], Cristtel Y. Ramirez-Corral[a], Michael Bass[b], Ying Chen[b], Young Key Kwon[a], [a]Powerlase Photonics Ltd., Units 3 & 4 Meadowbrook Industrial Estate, Maxwell Way, Crawley, RH10 9SA, United Kingdom; [b]CREOL, The College of Optics and Photonics, University of Central Florida, Orlando, FL 32816, USA

ABSTRACT

A high-power green picosecond laser based on the 'Z-slab' Nd:YAG amplifier is presented. The edge-pumped zigzag amplifier was designed to achieve high energy scaling with good beam quality. In a master oscillator power amplifier system 120 W average power was produced at 1064 nm, which was frequency doubled to 84 W at 532 nm. The maximum pulse energy was 400 µJ at 1064 nm and 280 µJ at 532 nm. The repetition rate was variable from 250 to 1000 kHz with M^2 < 1.4. In burst mode with 1-10 pulses, over one millijoule total burst energy was demonstrated at 1064 nm.

Keywords: Picosecond, ultrafast lasers, second harmonic conversion, multi-pass zigzag slab amplifier, burst mode, Z-slab.

1. INTRODUCTION

Ultrashort pulse lasers are increasingly being used in industrial micromachining applications. If the energy is sufficiently high, picosecond lasers can achieve cold ablation, enabling high-quality micromachining with minimal heat affected zones[1]. Ultrashort lasers are particularly useful for machining of materials such as glass and sapphire. Transparent materials are difficult to machine with nanosecond lasers in the visible and near-infrared, while the long pulse durations of CO_2 lasers cause excessive heating. By contrast, high-energy ultrashort lasers can exceed the electrical breakdown threshold to achieve efficient, high-quality machining. To maximize the intensity, both high energy and low M^2 are crucial parameters. Visible or ultraviolet wavelengths are also desirable because the higher photon energy aids absorption and allows focusing to smaller spot sizes.

In designing high-energy ultrashort pulses lasers, one of the critical limitations is nonlinear effects. Accumulation of nonlinear phase (quantified by the B-integral) can lead to critical self-focusing, which ultimately limits the energy scalability of ultrafast amplifiers. This effect is particularly strong in fiber lasers owing to their small core size and long interaction length. Much research has focused on overcoming these problems in fiber amplifiers using techniques such as chirped-pulse amplification, photonic crystal fibers[2], and spatial[3] or temporal[4] multiplexing. Bulk solid-state amplifiers, such as the thin disk[5] and Innoslab[6] designs, have proved particularly effective for scaling ultrashort pulse lasers to the multi-hundred microjoule level and beyond.

The zigzag based amplifier design[7-9] has been shown to be a promising power amplifier for high-power, high-energy picosecond laser systems. A variant of the zigzag scheme named the Z-slab was presented in our previous work, in which a picosecond laser was power scaled up to 150 W[10]. However, while both high energy (> 400 µJ) and low M^2 were demonstrated, achieving them simultaneously was not straightforward. The dual goals of high beam quality and low B-integral are affected in different ways by the various parameters of the slab design, so careful optimization is required to achieve the desired performance.

In this work, we present a Z-slab amplifier that has been designed to minimize the B-integral and allow high energy scaling without sacrificing beam quality. A multi-stage modular master oscillator power amplifier (MOPA) system based on this slab is presented and characterized. The effect of the amplifier chain on bursts of picosecond pulses is shown, and efficient second harmonic generation is demonstrated.

[*] s.chard@powerlase-photonics.com; tel +44 (0)1293 456 222; fax +44 (0)1293 456 235; powerlase-photonics.com

2. SLAB DESIGN

The Z-slab amplifier developed for this work is shown schematically in fig. 1 (a). The Z-slab is a high aspect ratio zigzag slab of 1 at.% Nd:YAG, which is edge-pumped through the two long side faces and cooled through the two large top and bottom faces. The beam to be amplified passes through the two small end faces, which are Brewster cut. The Brewster angle causes the beam to refract and follow a zigzag path with many total internal reflections against the two large faces. The slab was pumped by a pair of diode bar arrays at 885 nm, arranged opposite each other. The long edge faces were antireflection (AR) coated at 885 nm.

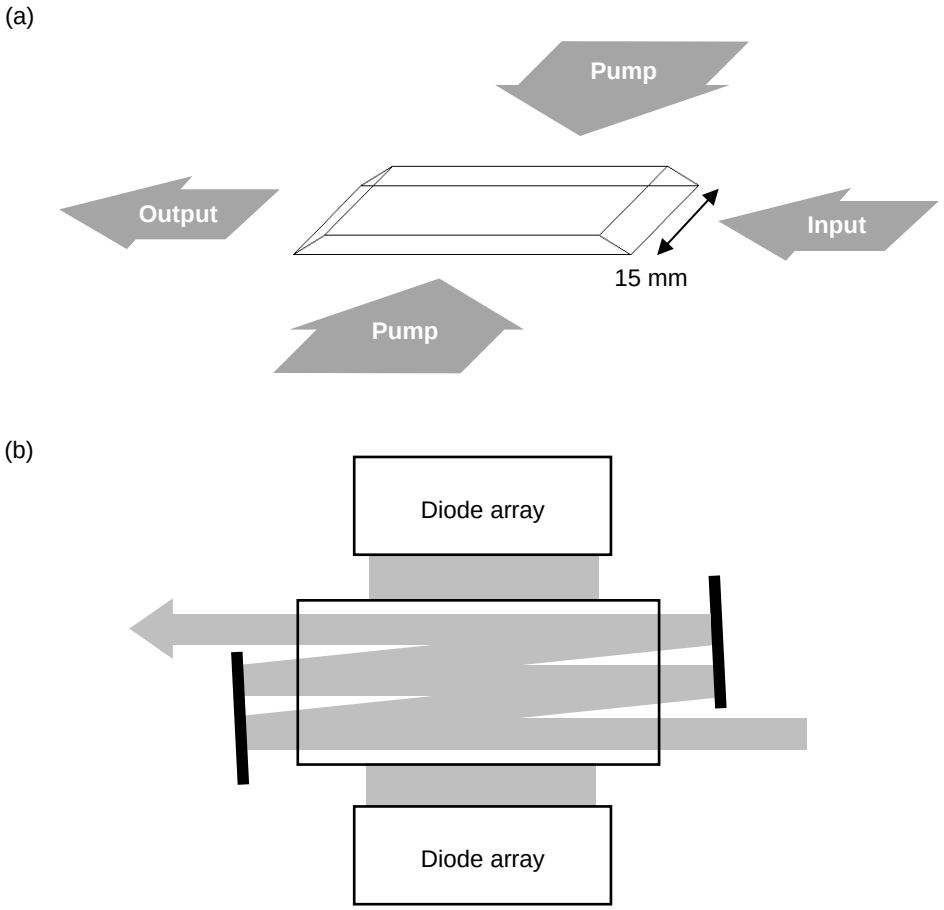

Figure 1. Schematic of Z-slab showing (a) slab shape and (b) multi-pass configuration.

As shown in fig. 1 (b) the beam makes multiple spatially-separated passes through the slab. In our previous work it was found that this substantially reduces the impact of thermal lensing and gain non-uniformity in the amplifier[10]. With multiple passes, the beam experiences spatial averaging along the horizontal axis in an analogous way to the effect of the zigzag path in the vertical axis.

This work was based on a wide version of the Z-slab amplifier designed specifically for high-energy operation. The 15 mm diameter allowed the use of a large beam diameter together with multiple passes. The width of the slab also helped to simplify the Z-slab design, as there was sufficient single-pass pump absorption so that a double-pass pumping scheme was not necessary.

3. EXPERIMENTAL SET-UP

Two Z-slab amplifier modules were combined in an amplifier chain as shown in fig. 2. The seed laser was a commercial picosecond laser system with 8.5 ps pulse duration. The repetition rate of the seed laser was variable from 100 – 1000 kHz with constant average power. This was combined with a proprietary pre-amplifier to give up to 35 W average power. The energy after pre-amplification was limited to a maximum of 120 μJ to avoid nonlinear effects in the pre-amplifier. A spatial filter was applied after the pre-amplifier to remove beam distortions, after which the M-squared was between 1.12 and 1.30, depending on the repetition rate.

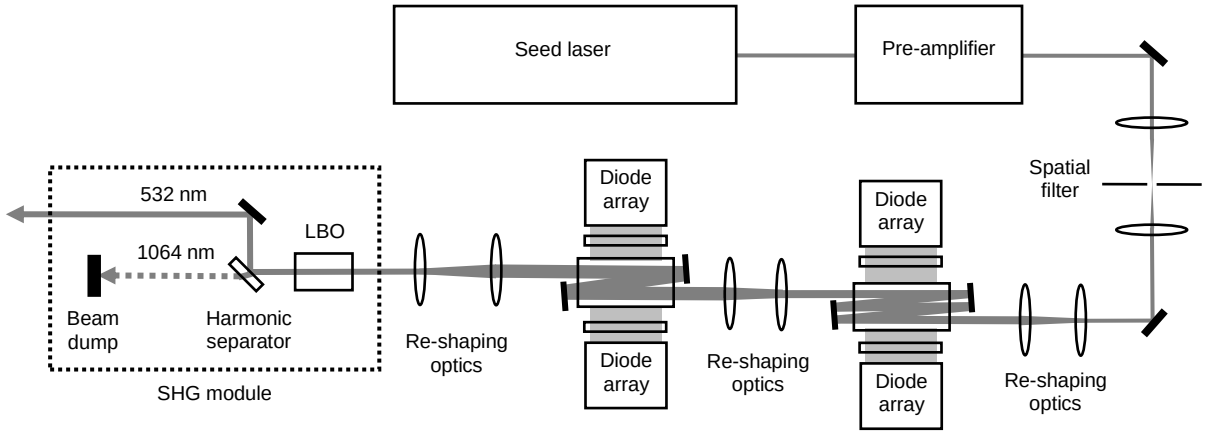

Figure 2. Schematic diagram of MOPA system with second harmonic generation.

Before it was input to the first Z-slab, the beam was re-shaped to have a $1/e^2$ diameter of 2.5 x 1.1 mm in the horizontal (along the pumping direction) and vertical (along the slab thickness) axes respectively, and re-shaped again to 4.0 x 1.1 mm for the second amplifier. The beam made five passes of the first amplifier and three passes of the second amplifier.

A second harmonic generation (SHG) module was attached to the end of the laser. This contained a Lithium Triborate (LBO) crystal operated in type I critically phase matched configuration at a temperature of 50 °C. The residual infrared light was filtered out by a dichroic harmonic separator mirror. The beam into the SHG module was re-shaped to be circular with a diameter of 1.5 mm.

4. RESULTS

4.1 Infrared system

The laser system was first characterized without the SHG module. Figure 3 shows the output power vs absorbed pump power per amplifier. Up to 130 W average power was produced with both Z-slab amplifiers pumped at 520 W absorbed pump power. Although the diode arrays were capable of delivering more power, the pump power was limited to this level in order to preserve the beam quality.

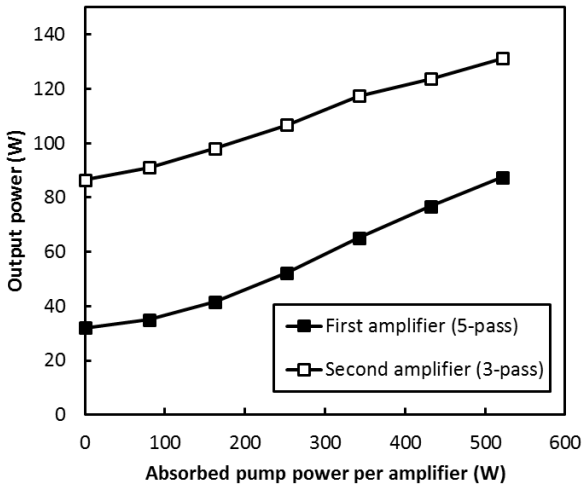

Figure 3. Power curves for both Z-slab power amplifiers at 400 kHz repetition rate.

The performance was characterized as a function of seed laser repetition rate between 250 – 1000 kHz. To avoid the risk of damage in the pre-amplifier, the seed laser was not operated under 250 kHz. Figure 4 shows the average power and pulse energy as functions of repetition rate. Up to 400 µJ was obtained at 250 kHz. Since the average power from the seed laser was constant, the pulse energy was approximately inversely proportional to the repetition rate. At low repetition rates however there was a drop in average power. The reason for this was that the seed laser and pre-amplifier produced poorer beam quality at low repetition rates, and this resulted in more power being removed by the spatial filter.

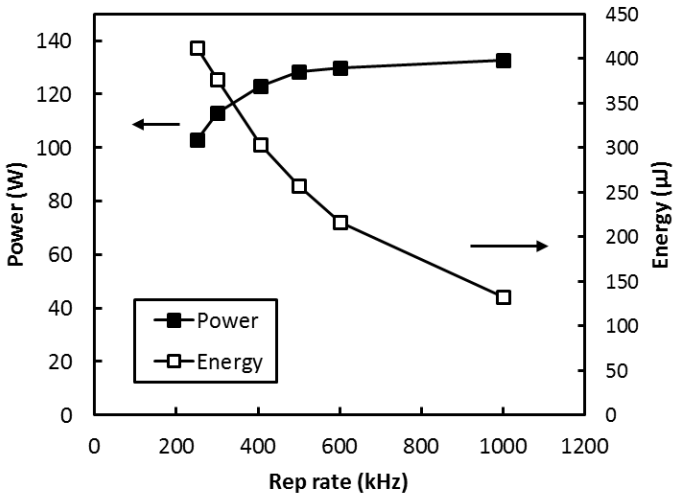

Figure 4. Average power and pulse energy as functions of repetition rate.

Figure 5 (a) shows the horizontal and vertical beam caustics used to measure the beam quality, along with the beam profile at the waist position. This measurement was taken with both amplifiers at full power and the seed laser at 400 kHz repetition rate. Along both axes a value of $M^2 < 1.30$ was measured. Figure 5 (b) shows the beam quality as a function of repetition rate. Both M_x^2 and M_y^2 remained below 1.4 across the range, showing that the slab design was successful at maintaining high beam quality while amplifying picosecond pulses to high energies. The beam circularity

and astigmatism after the beam re-shaping optics were also observed. Across the full repetition rate range the beam circularity remained over 90%, and the astigmatism was under 10 %.

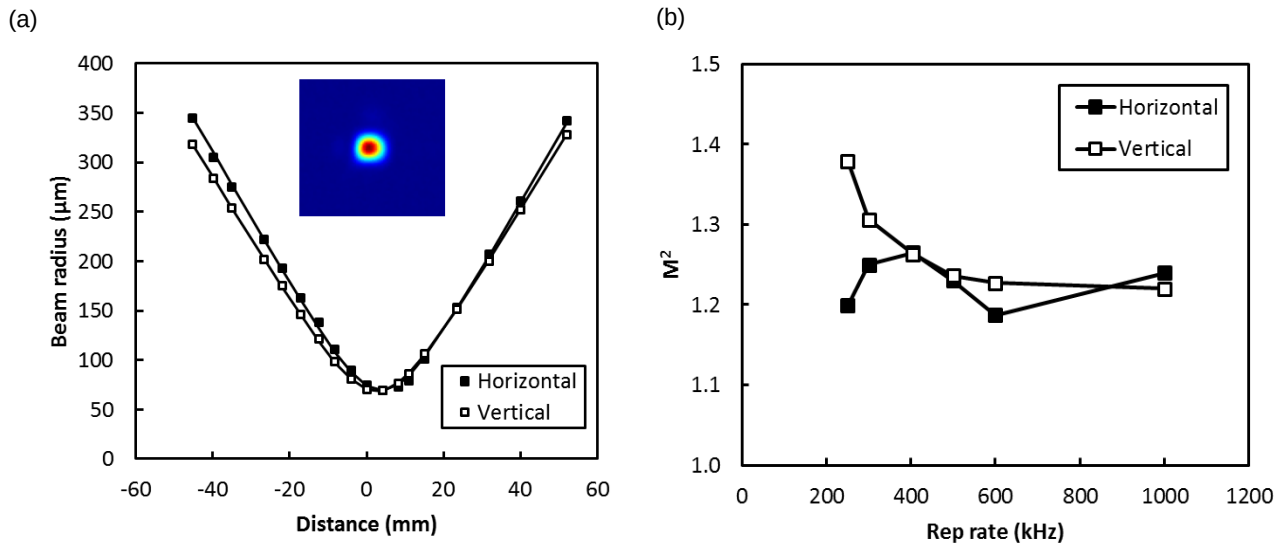

Figure 5. (a) Horizontal and vertical caustics at maximum power and 400 kHz repetition rate (M_x^2, M_y^2 < 1.30) with beam profile at the waist position (inset) and (b) M^2 vs repetition rate at full pump power.

An autocorrelation measurement was made of the laser output. The seed laser had a pulse duration of 8.5 ps. Under amplification the pulse duration increased to 8.8 ps at 1000 kHz and 9.4 ps at 250 kHz.

4.2 Burst mode

The seed laser had the capability to operate in 'burst mode'. It contained an internal fiber oscillator mode-locked at a fixed frequency of 30 MHz, which was pulse picked at the desired repetition rate. By increasing the duration of the pulse picker window, a burst of pulses could be extracted each period. The number of pulses per burst could be varied from 1 – 10.

Figure 6 shows two examples of amplified bursts measured on a photodiode. By default the burst from the seed laser was flat (all pulses in the burst contained equal energy), and in most cases the burst remained flat during amplification. At low repetition rates however, the effect of saturation in the amplifiers caused some distortion in the relative pulse heights, which was partially corrected by appropriately pre-shaping the burst from the seed laser.

Since the energy was spread across multiple pulses, it was possible to operate at lower repetition rates in burst mode than in single pulse operation (and thus achieve higher total energies). Figure 7 shows the total burst energy as a function of repetition rate, which peaked at 1.1 mJ at 100 kHz. To avoid the risk of damage in the pre-amplifier, the minimum number of pulses per burst was limited so that the energy of the individual pulses remained below 400 µJ.

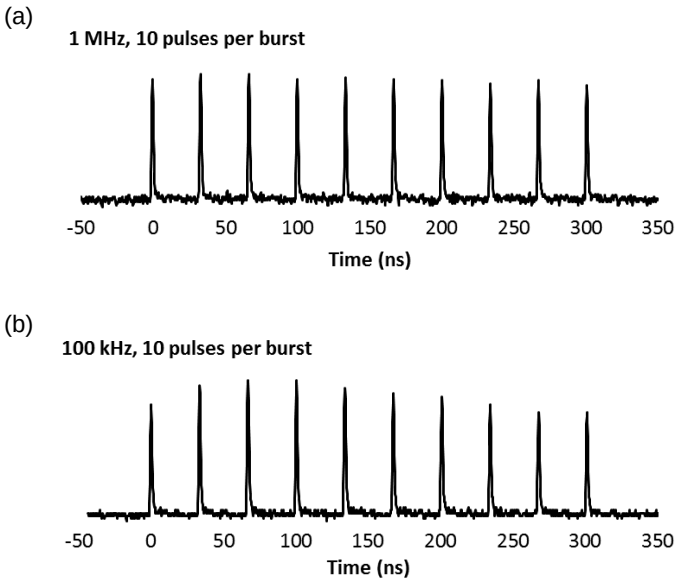

Figure 6. Amplified burst pulse traces with 10 pulses per burst at (a) 1 MHz and (b) 100 kHz repetition rate.

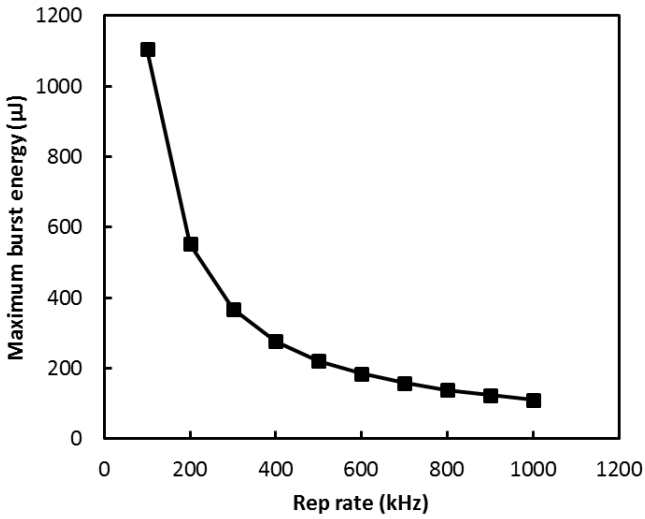

Figure 7. Maximum total burst energy as a function of repetition rate.

4.3 Second harmonic generation

After re-shaping, the beam was passed through the SHG module, and the converted 532 nm power was measured after the harmonic separator. The laser was operated at repetition rates from 300 to 1000 kHz, and the green power and conversion efficiency are plotted in fig. 8. A maximum of 84 W average power was obtained at 532 nm with 400 kHz repetition rate. This was achieved with a conversion efficiency of 70%. The highest energy was 280 µJ, which occurred at 300 kHz. No significant increase in the M^2 was observed in the 532 nm beam relative to the input 1064 nm beam.

The lower conversion efficiency at 300 kHz was likely due to the higher M^2 of the IR beam at low repetition rates. Since the system was optimized for conversion efficiency at low repetition rate (for high energy), it did not convert as well at

high repetition rates. It is likely that higher conversion efficiency could have been achieved at high repetition rates with suitable beam shaping.

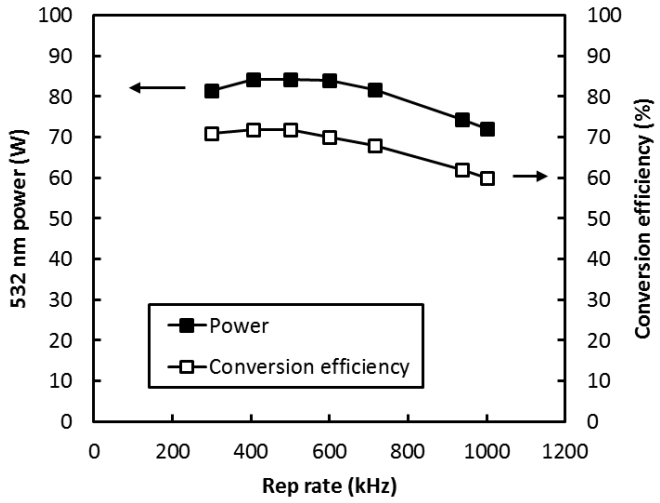

Figure 8. Power at 532 nm and conversion efficiency as a function of repetition rate for laser system with SHG module.

5. CONCLUSION

In summary, we have demonstrated a green picosecond laser system based on the Z-slab Nd:YAG amplifier which combines high-energy amplification with high beam quality. The edge-pumped zigzag amplifier was designed to minimize the B-integral while incorporating multiple spatially-separated passes to preserve beam quality. Up to 120 W average power was produced at 1064 nm, with a maximum energy of 400 µJ. The repetition rate was variable from 250 to 1000 kHz with $M^2 < 1.4$. In burst mode with 1-10 pulses, over one millijoule total burst energy was demonstrated at 1064 nm. When the output was frequency doubled with an LBO crystal, up to 84 W average power at 532 nm was obtained, with a maximum energy of 280 µJ.

REFERENCES

[1] Liu, X., Du, D. and Mourou, G., "Laser ablation and micromachining with ultrashort laser pulses," IEEE J. Quant. Electron. 33(10), 1706-1716 (1997).

[2] Wan, P., Yang, L.-M. and Liu, J., "All fiber-based Yb-doped high energy, high power femtosecond fiber lasers," Opt. Express 21(24), 29854-29859 (2013).

[3] Klenke, A., Seise, E., Demmler, S., Rothhardt, J., Breitkopf, S., Limpert, L. and Tünnermann, A., "Coherently-combined two channel femtosecond fiber CPA system producing 3 mJ pulse energy," Opt. Express 19(24), 24280-24285 (2011).

[4] Kienel, M., Klenke, A., Eidam, T., Hädrich, S., Limpert, J. and Tünnermann, A., "Energy scaling of femtosecond amplifiers using actively controlled divided-pulse amplification," Opt. Lett. 39(4), 1049-1052 (2014).

[5] Negel, J.-P., Loeschner, A., Voss, A., Bauer, D., Sutter, D., Killi, A., Ahmed, M. A. and Graf, T., "Ultrafast thin-disk multipass laser amplifier delivering 1.4 kW (4.7 mJ, 1030 nm) average power converted to 820 W at 515 nm and 234 W at 343 nm," Opt. Express 23 (16), 21064-21077 (2015).

[6] Russbueldt, P., Hoffman, D., Höfer, M., Löhring, J., Luttmann, J., Meissner, A., Weitenberg, J., Traub, M., Sartorius, T., Esser, D., Wester, R., Loosen, P. and Poprawe, R., "Innoslab amplifiers," IEEE J. Sel. Top. Quantum Electron. 21(1), 447-463 (2015).

[7] Goodno, G. D., Palese, S., Harkenrider, J. and Injeyan, H., "Yb:YAG power oscillator with high brightness and linear polarization," Opt. Lett. 26(21), 1672-1674 (2001).

[8] Chen, B., Dong, J., Patel, M., Chen, Y., Kar, A. and Bass, M., “Modeling of high power solid-state slab lasers,” Proc. SPIE 4968, 1-10 (2003).
[9] Chen, J., Li, J., Xu, J., Liu, W., Bo, Y., Feng, X., Xu, Y., Jiang, D., Chen, Z., Pan, Y., Guo, Y., Yan, B., Guo, C., Yuan, L., Yuan, H., Lin, Y., Xiao, Y., Peng, Q., Lei, W., Cui, D. and Xu, Z., "4350W quasi-continuous-wave operation of a diode face-pumped ceramic Nd: YAG slab laser," Optics & Laser Technology 63, 50-53 (2014).
[10] Kwon, Y. K., Chard, S. P., Hay, N., Rodin, A. M., Bass, M., Chen, Y., Shu, H. and Webster, S., “200W output power at 10ps from a scalable Z-slab Nd: YAG laser,” Proc. SPIE 8959, 89590V (2014).